

Micro-structuring of tungsten for mitigation of ELM-like fatigue

A Terra¹ , G Sergienko , M Gago , A Kreter , Y Martynova, M Rasiński , M Wirtz , Th Loewenhoff , Y Mao , D Schwalenberg, L Raumann , J W Coenen , S Moeller, Th Koppitz, D Dorow-Gerspach, S Brezinsek , B Unterberg  and Ch Linsmeier 

Forschungszentrum Jülich GmbH, Institut für Energie- und Klimaforschung, Partner of the Trilateral Euregio Cluster (TEC), 52425 Jülich, Germany

E-mail: a.terra@fz-juelich.de

Received 28 June 2019, revised 11 October 2019

Accepted for publication 16 October 2019

Published 6 March 2020



CrossMark

Abstract

Fusions reactors have to handle numerous specifications before being able to show viable commercial operation, one of which is to find a proper Plasma Facing Material (PFM) which can withstand the high heat loads of several tens of megawatts per square meters combined with the pulse operation of a tokamak and many other problematics (Brezinsek *et al* 2017 *Nucl. Fusion* **57** 116041). Nowadays, only tungsten is considered as a PFM for high heat flux areas of a tokamak divertor. Tungsten has been selected due to its favorable physical properties, but tungsten has a major drawback: it is brittle under temperatures typically used for water-cooled plasma-facing components (PFC). Under these temperatures the damage threshold due to thermal fatigue induced by ELM is very low, which will dramatically reduce the life-time of the tungsten PFC. The ANSYS simulations and experiments with a millisecond pulsed laser demonstrate a strongly improved ability to withstand thermal fatigue by micro-structuring of the tungsten surface with the help of 150–240 μm diameter tungsten fibres.

Keywords: tungsten, fusion, plasma-facing component, micro structure, thermal stress, heat load, ITER

(Some figures may appear in colour only in the online journal)

1. Introduction

Tokamaks, which were invented in the 50s, are one of the most studied ways of achieving controlled fusion reaction with power generation in mind. However, due to high electrostatic repulsion forces, bringing two nuclei together to fuse into a bigger one, while releasing energy due to the difference in masses between reactants and products, implies, in most cases, very high temperatures. These temperatures of about ten millions of Kelvins in the centre of the Sun need to be increased by another factor of ten in tokamaks because of the comparatively lower density. At such temperatures, reactants and products are under the form of plasma, and are kept away from the reactor wall by magnetic confinement. Still, the wall receives a major fraction of injected and released energy by direct heat radiation and also by intensive

particle bombardment, with a magnitude of the order between 10 MW m^{-2} (average) to 1 GW m^{-2} (short term events like edge-localized modes (ELMs) or electron runaway).

Both the intersect pulse operation of tokamaks and the repetitive short term events make it a necessity for the first wall material to have strong thermal cycling capabilities. Tungsten has been mainly selected so far because of its highest melting point of all metals, pretty low hydrogen (and tritium) retention and low sputtering regarding particle bombardment [1]. However, it has a major drawback—its propensity to crack under repeated thermal loads. This is mainly due to its low ductility, which also may lead to possible catastrophic failures without warning, which is a serious issue in a fusion reactor.

The materials science community addressed this issue by trying to add some ductility (or pseudo ductility) by alloying tungsten with other elements [2], by compositing it with fibres [3] or by controlling its granular structure. Unfortunately, all

¹ Author to whom any correspondence should be addressed.

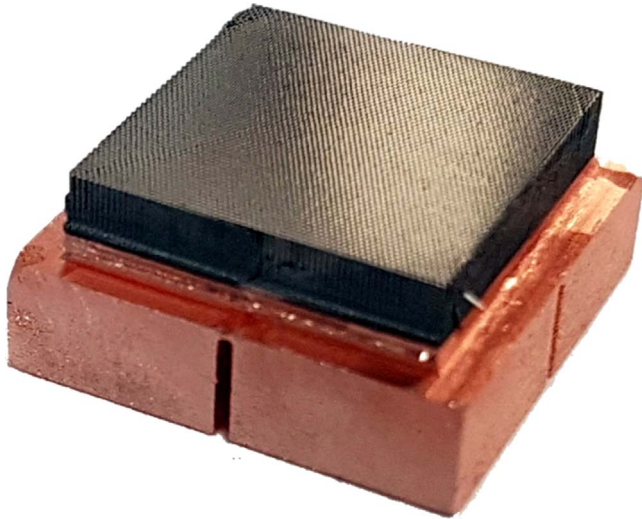


Figure 1. The sample contains about 5000 fibres of $150\ \mu\text{m}$ diameter forming a square of $10 \times 10\ \text{mm}$ implemented in a copper heatsink of $12 \times 12\ \text{mm}$.

these methods may be countered in time by the neutron irradiation that occurred during fusion, as it may significantly change their composition (due to transmutations), and also because of other factors (recrystallization by operational temperature peaks, helium embrittlement ...). In the present article, the authors tried to mitigate the stresses induced by the loads applied on first wall material by means of micro-castellation. By reducing loads on the plasma-facing material (PFM), with the advantage of removal of the need for higher ductility, tungsten can be used as it is. The whole concept behind micro-structured tungsten, its possible benefits and all initial experimental parameters have been described in a previous paper [4]. It was shown that the power handling, the erosion and the fuel retention, within the experimental boundary conditions, were comparable to ITER-grade bulk tungsten. However, the thermal fatigue withstanding capabilities of micro-structured samples was revealed to be much higher than its reference bulk tungsten counterpart.

2. Combined sequential deuterium plasma followed by laser irradiation

2.1. Pyrometer measurements

The previous SEM inspections [4] revealed the absence of any damage on the micro-structured sample after 10^5 heat pulses, while cracking, roughening and melting appeared on the bulk reference sample after only ten pulses of the same intensity [4].

These first results could be confirmed by further analysis of the recorded experimental data, as the pyrometer trace showed that the surface temperature of the $\text{Ø}150\ \mu\text{m}$ fibre (2.4 mm long) micro-structured sample, shown in figure 1, remained stable (once it passed a short thermal transient phase), while the surface temperature of the reference sample was constantly increasing with the number of pulses up to 10^4

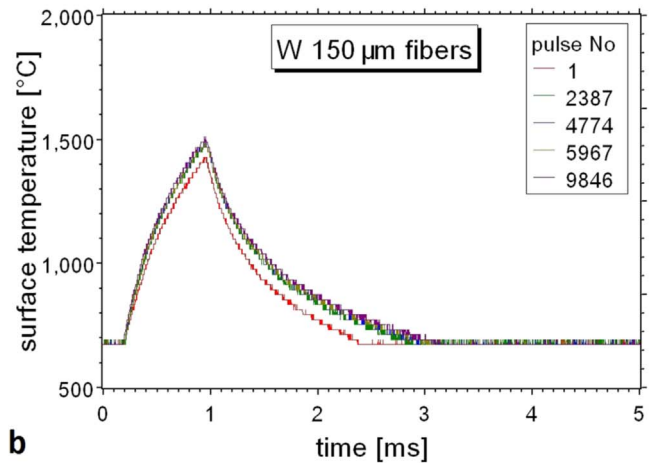
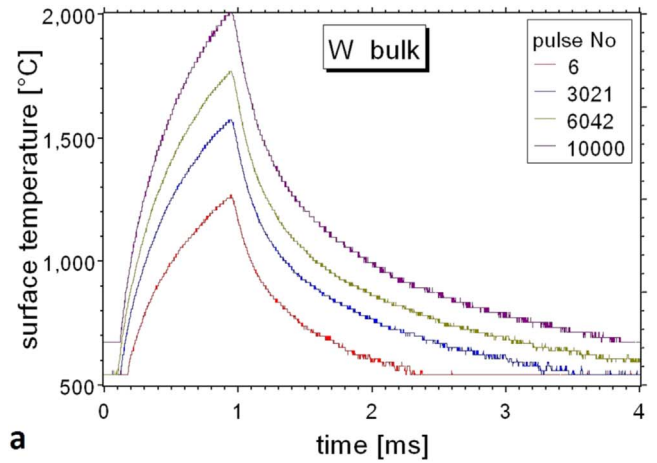


Figure 2. Surface temperature temporal profiles of the bulk reference sample (a) and the micro-structured sample (b) measured by pyrometer at different pulse numbers.

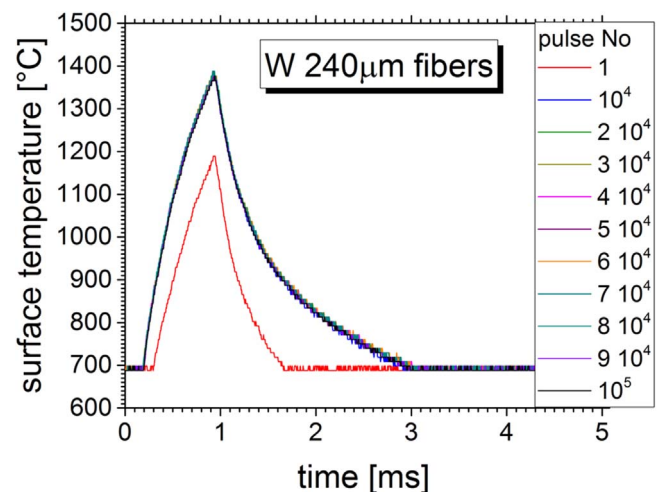


Figure 3. Surface temperature temporal profiles of micro-structured sample produced from $\text{Ø}240\ \mu\text{m}$ fibres along 10^5 laser pulses of $0.5\ \text{GW m}^{-2}$.

pulses of $0.64\ \text{GW m}^{-2}$, as seen in figure 2. This is because of surface damage and an increase in roughness that increase the absorbed energy amount from the laser pulse with constant power. This increase in the absorption coefficient in the laser

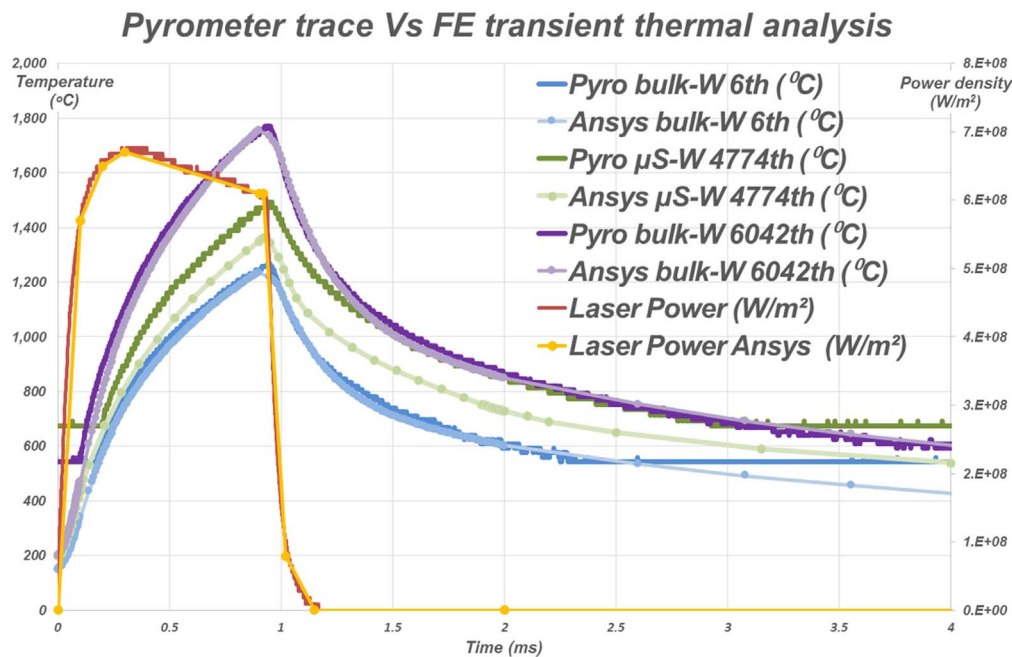


Figure 4. Sample surface temperature temporal profiles of bulk and micro-structured samples measured by pyrometer and fitted with the help of ANSYS simulations.

spot area is also visible on a metallographic microscope micrograph, as a dark area.

The same behaviour was observed with another micro-structured sample made of larger $\text{\O}240 \mu\text{m}$ fibres. The surface temperature's temporal profile and peak value inside the laser spot does not change from 10^4 to 10^5 pulses at the power density of 0.5 GW m^{-2} ($\lambda = 1064 \text{ nm}$, $d = 3 \text{ mm}$), as shown in figure 3, because no surface degradation occurs, which could increase surface emissivity and absorption of the laser beam energy. The surface temperature measurements are consistent with the SEM observation reported in [4].

2.2. Finite element method (FEM) thermal transient analysis with ANSYS.

Using the results shown in figure 2, a transient thermal analysis including a fit was performed with the help of an ANSYS code and 3D design software. For the calculations, the same thermal dependent thermal and mechanical material properties of tungsten were used for both bulk tungsten and tungsten fibre. For the micro-structured sample, pure copper properties were used to simulate the effect of the heatsink. The environment temperature was set to a steady-state temperature measured during the experiment [4] to take into account transient effects. The laser pulse energy absorbed by the sample was defined by the emissivity coefficient. The analysis was performed to estimate the change in the emissivity coefficient of the bulk tungsten sample between the 6th pulse after the transient phase and the 6042th. ANSYS calculations show that the emissivity at the laser wavelength ($\lambda = 1.064 \mu\text{m}$) was increased by about 30%, as seen in figure 4.

The calculations showed that the emissivity coefficient is correlated with the progressive increase in surface damages,

turning the electro-polished surface of the reference sample into a heavily damaged surface by surface roughening and cracking, which is visible both under SEM [4] or optical microscopy. The increase in the surface damage results in the enhanced absorption of the laser pulse, and accordingly, the increase in the surface temperature.

3. Tungsten fuzz on micro-structured tungsten and laser irradiation

To confirm the previous experimental results and the improvement factor of at least 10^5 in fatigue over bulk tungsten that was observed in [4], it was decided to set up another experiment, similar to the protocol and goal [5, 6] but using different physical parameters.

3.1. Reproducibility of previous results

The same PSI-2 linear machine [7] was operated with a deuterium plasma with 6% helium (80 and 20 sccm for deuterium gas and helium gas flows, respectively). The total ion flux on the samples was about $7.3 \times 10^{21} \text{ m}^{-2} \text{ s}^{-1}$ for a total fluence of about $8.5 \times 10^{25} \text{ m}^{-2}$ on the reference sample and exactly double (due to exposure time) for the micro-structured sample. The helium and deuterium mixed plasma at the ion energies of about 100 eV (due to the samples' biasing) present the advantage of producing surface modifications of exposed tungsten samples with the formation of nano-structures called 'fuzz' [8]. These structures can become molten/sublimated under high heat flux like those produced by the additional laser irradiation (which was performed sequentially after plasma exposure). The other main difference is the range of the steady-state temperature, which was significantly

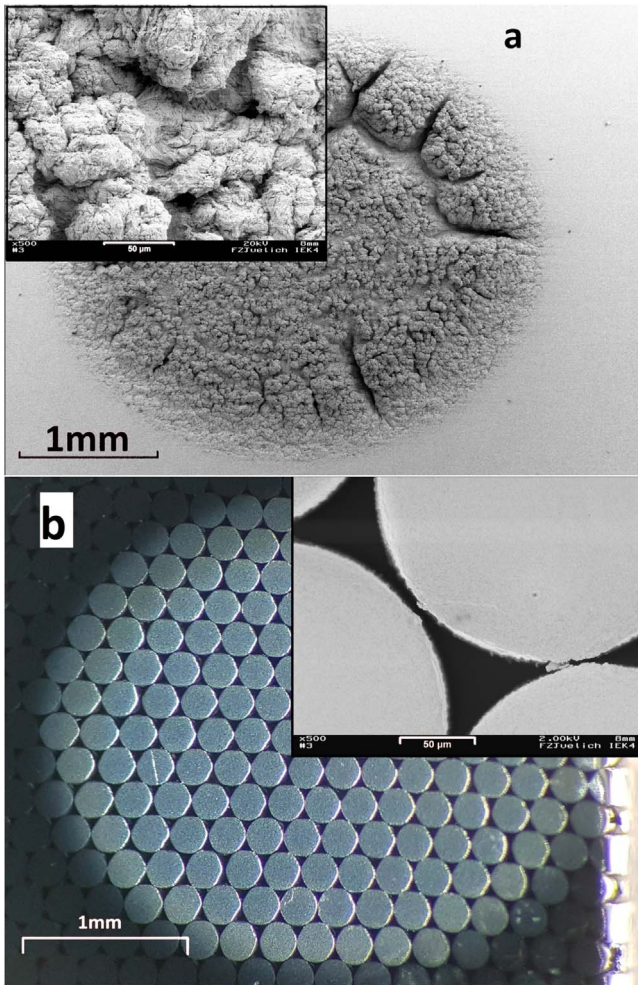


Figure 5. (a) A surface micrograph of the bulk reference sample (left, SEM) after 10^5 laser pulses, and (b) the micro-structured sample (right, optical) after 10^5 and $7 \cdot 10^4$ laser pulses, respectively.

higher ($700\text{ }^{\circ}\text{C}$ – $800\text{ }^{\circ}\text{C}$) than in the previous experiment [4] ($150\text{ }^{\circ}\text{C}$ – $250\text{ }^{\circ}\text{C}$). A detailed description about fuzz phenomenon and reference bulk sample behaviour can be found in (Gago PFMC 2019, proceeding). One of the main advantages of the fuzz presence is the possibility of visualising the laser irradiation area by the melt/sublimation of the fuzz, which can be detected with both SEM and optical microscopes, while fuzz do not prevent or interfere with the typical thermal shock damages (roughening, crack, recrystallisation or melt) in the near surface layer, as it is visible on the bulk sample.

The previous results shown in [4] were confirmed despite the breakdown of the laser, which resulted in the micro-structured sample being exposed to $7 \cdot 10^4$ laser pulses, which is less in comparison with the 10^5 laser pulses of the bulk sample exposure. Figure 5 clearly shows the exact same type of damage on the bulk reference sample (figure 5(a)) and the total absence of any damage visible (up to resolutions of 5 nm/pixel) on the micro-structured one (figure 5(b)), in the exact same pattern as was shown in [4]. The reference sample shows deep cracking, roughening of its surface, recrystallization and melting of sharp edges, while the micro-structured

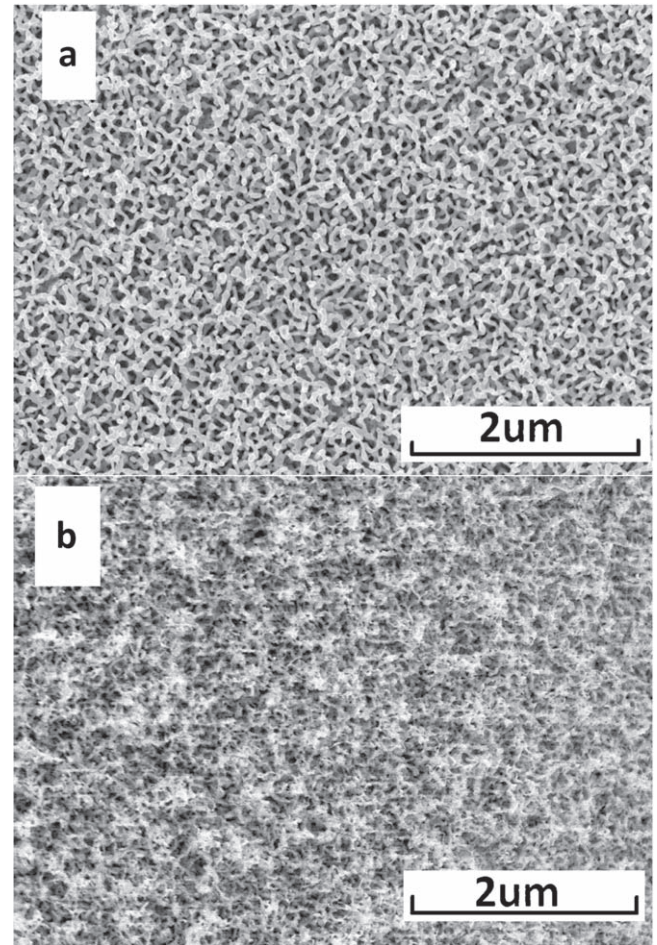


Figure 6. The fuzz structure of (a) the bulk tungsten reference sample and of (b) the micro-structured sample after only plasma irradiation of a D_2/He mixture with ion energy of 100 eV .

sample did not show any of these changes, despite comparison of pre- and post-experimental micrographs through a full mapping of its surface at a resolution of $20\text{ }\mu\text{m}$ (in addition to the local SEM pictures at higher resolution).

3.2. Tracing fuzz melting

The creation of fuzz allowed us to trace the laser irradiation as the fuzz melted and/or sublimated. This is clearly visible on the macroscopic scale as fuzz has strong light absorption and appears dark (figure 5(b)), and has a typical structure easily recognizable by SEM, as seen in figure 6.

The SEM analysis shows that the fuzz is slightly wider (about 34 nm) on the bulk reference sample (figure 6(a)) in comparison with the micro-structured sample (about 19 nm) (figure 6(b)), while the plasma parameters were the same. This difference could be due to the differences in the original grain sizes and shapes of the two samples ($1\text{--}10\text{ }\mu\text{m}$ for the bulk sample, and $0.2\text{--}1\text{ }\mu\text{m}$ for the fibres, [4]).

As foreseen, the melting of fuzz allows us to precisely determine the area of the laser irradiation by the surface modification (figure 7(a)). Due to the fibres' insulation relative to the others, it is even possible to spot the transition

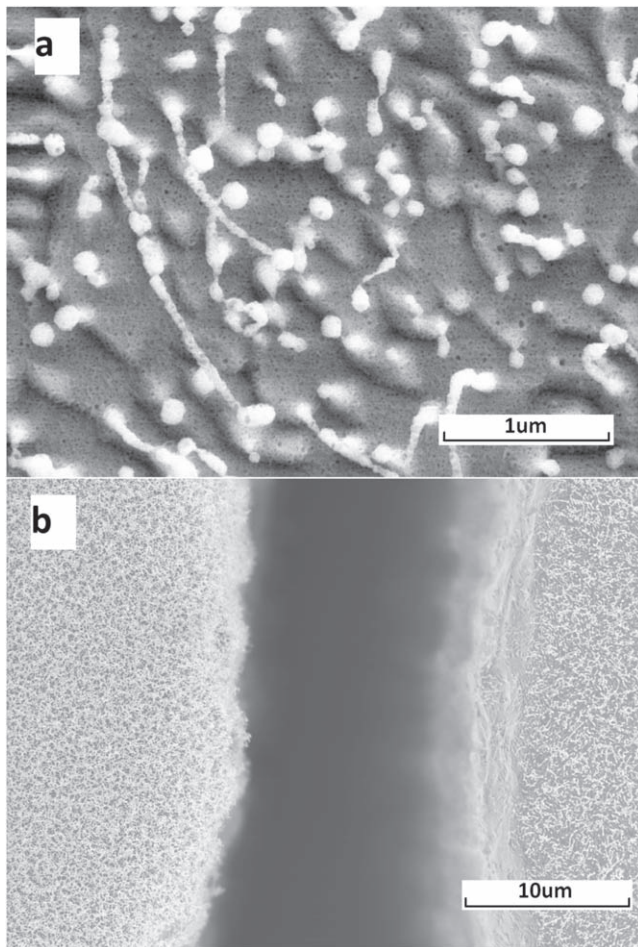


Figure 7. The molten fuzz structure of (a) the micro-structured sample and (b) laser irradiation transition between two fibres.

between two fibres (figure 7(b)), when the power density reaches the fuzz's damage threshold on one fibre (right) but not on its direct neighbour (left). This method allowed us to track down laser irradiation on the micro-structured sample because the laser irradiated area is clearly visible in both visible light microscopy and SEM. While this paper focus on micro-structured sample, a detailed review of reference sample is available in [9].

4. Exploring thermal fatigue capabilities

One can argue that an improvement by a factor of 10^5 in the thermal fatigue resistance of the micro-structured sample could come from the extraordinary property of the fibre material due to the thinner tungsten grain structure but does not come from the micro-structuring. Such a case would be problematic as it would make the micro-structuring a non-durable solution regarding recrystallization or transmutation, as previously discussed. The following specific experiment was performed to check the influence of the grain size of the fibres on the thermal fatigue ability of the micro-structured sample.

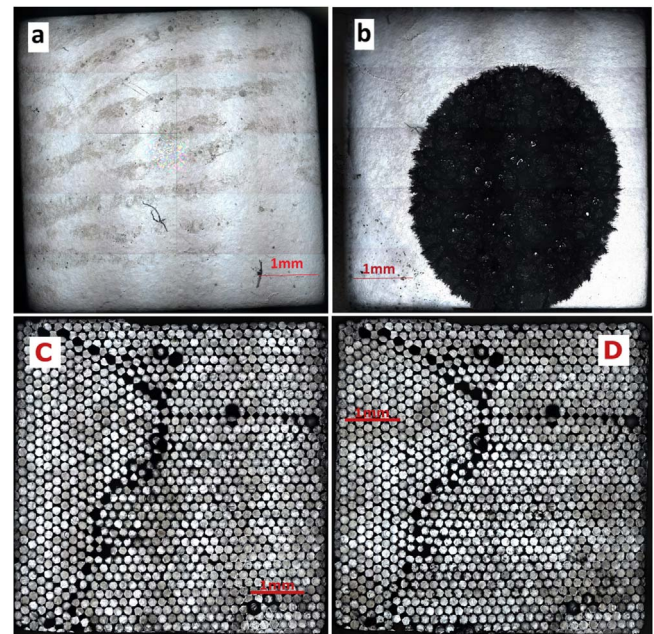


Figure 8. Metallographies of the reference bulk (top, (a) before and (b) after plasma and laser irradiation) and micro-structured sample (bottom, (c) before and (d) after plasma and laser irradiation). Pyro μ S-W 4774th ($^{\circ}$ C).

4.1. Recrystallized fibres sample

The same $\text{\O}150 \mu\text{m}$ fibres previously used [4] were recrystallized during 5 h at 2000°C , which brought their average (transversal) grain size from an average size of $510 \pm 6 \text{ nm}$ to an average of about $1.35 \pm 0.33 \mu\text{m}$, which is similar to the grain size found in the bulk tungsten sample. Fibres were assembled in a $5 \times 5 \text{ mm}$ sample, and the fatigue experiment described in [4] was reproduced (sequential deuterium plasma exposure followed by 10^5 laser pulses at 0.50 GW m^{-2}).

While these results are still preliminary, the metallographic pictures presented in figure 8 verify the absence of damage visible at the macroscopic levels, which need to be confirmed at higher resolution by SEM. However, the difference from the heavily damaged reference bulk tungsten sample is very noticeable.

4.2. Mitigating thermal stress with micro-structuring

A derivative thermo-mechanical analysis from the transient thermal analysis described in section 2.2 was performed to evaluate the thermal stress induced by the laser irradiation pulses, as a representation of ELM-like events. The same power loading and induced temperatures that have been shown in section 2.2 were used. No residual stress was added from manufacturing (considered stress free at room temperature), and the volumes were clamped by using frictionless sliding contact (to avoid creating artificial stress concentration from thermal expansion).

It is clearly seen in figure 9 that von Mises normalised thermal stresses are reduced in the micro-structured tungsten in comparison with the bulk tungsten. The peak value is reduced from 1.5 GPa for the bulk tungsten sample to only 150 MPa for the tungsten fibre. The same is also valid for the

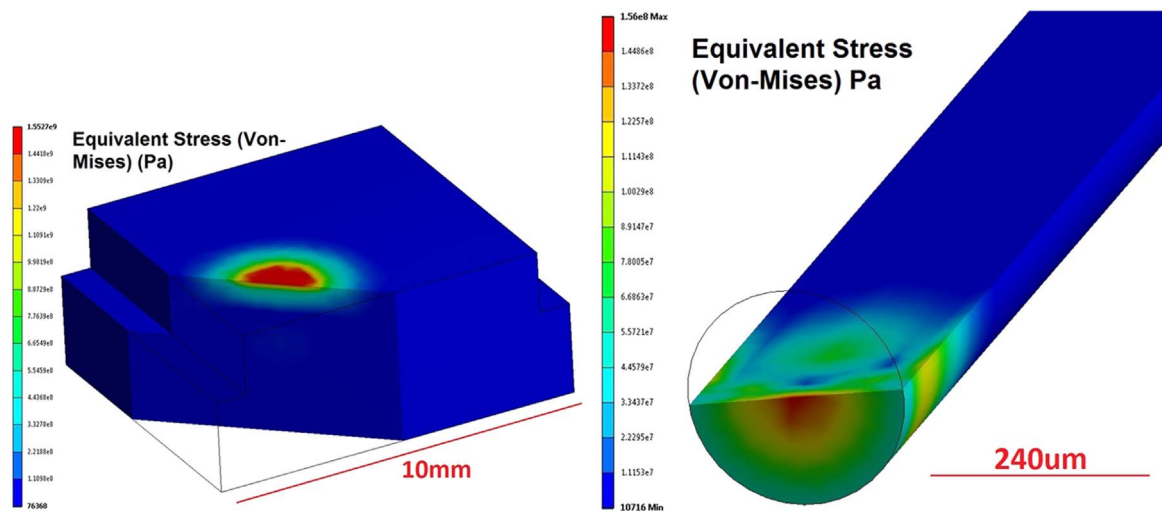


Figure 9. Peak thermal stress (von Mises) of the bulk reference sample (left) and an $\text{Ø}240 \mu\text{m}$ fibre (right) under an ELM-like event of 500 MW m^{-2} at 1 ms (the end of the laser pulse).

maximum principal stress that is also reduced from a range of 500 MPa for the bulk sample to about 50 MPa for the fibre. In both cases it corresponds to a factor of ten reduction in the induced thermal stress.

Additionally, it is interesting to consider the tungsten yield strength (YS) and ultimate tensile strength (UTS), which are, respectively, about 175 and 200 MPa for industrial grade tungsten at 1500 °C (and 75 and 125 MPa, respectively, when considering recrystallized tungsten) [4]. The results demonstrate that in the bulk sample, this limit is clearly overcome, which is the reason for the cracks and permanent damage. Meanwhile, for the fibre, we remain under YS, which means that it will be able to remain in the elastic domain and prevent the accumulation of plastic deformation. This calculation, besides its limitation, shows the evidence of the intersect mechanism that gives the micro-structured tungsten its thermal fatigue performance.

5. Conclusion

In this paper, further analysis of previous experimental results is reported [4]. The pyrometer measurements of the surface temperature evolution during laser pulses confirm the previous SEM observation of the absence of any surface damage of the micro-structured tungsten in contrast to the bulk tungsten samples.

All these results were also confirmed by a new experiment, which added fuzz creation to the experimental protocol to better characterise the laser irradiation at high energy densities. Put together, it confirms the considerable improvement ($+10^7\%$) that micro-structured tungsten represents over bulk tungsten, when considering thermal fatigue withstanding ability.

In addition, it was also confirmed that the improvement gain observed at first in a low temperature range (150 °C – 250 °C) is also observable at higher ranges (700 °C – 800 °C). This was expected and previously stated [4] because the lower temperatures present the most brittle scenario for tungsten.

The sample produced from recrystallized tungsten fibres has been tested by both plasma and laser loading. While still preliminary, the first result showed the absence of visible surface damage by optical microscopy. This observation confirms that the fibre material property cannot be considered as (fully?) responsible for the improved resistance of the micro-structured tungsten to thermal fatigue.

Transient thermo-mechanical analysis with ANSYS software has been coupled to the experimental results, and demonstrates the effectiveness of the micro-structuring and the reduction of thermal stress induced by ELM-like events by a factor of ten. When compared to the standard tungsten material properties (YS and UTS), it is possible to explain the previously observed improvement gains.

To finalise, let us be reminded that at least 10^8 type I ELM events with power densities up to 1 GW m^{-2} are foreseen for ITER, which allow one to have a perspective for the micro-structured plasma-facing components.

Acknowledgments

This work has been carried out within the framework of the EUROfusion Consortium, and has received funding from the Euratom research and training programme 2014–2018 and 2019–2020 under grant agreement No. 633053. The views and opinions expressed herein do not necessarily reflect those of the European Commission.

ORCID iDs

A Terra <https://orcid.org/0000-0003-0638-6103>
 G Sergienko <https://orcid.org/0000-0002-1539-4909B>
 M Gago <https://orcid.org/0000-0003-1553-0824>
 A Kreter <https://orcid.org/0000-0003-3886-1415>
 M Rasiński <https://orcid.org/0000-0001-6277-4421>
 M Wirtz <https://orcid.org/0000-0002-1857-688X>

Th Loewenhoff  <https://orcid.org/0000-0001-7273-4327>
Y Mao  <https://orcid.org/0000-0002-5518-2791>
L Raumann  <https://orcid.org/0000-0001-6043-7093>
J W Coenen  <https://orcid.org/0000-0002-8579-908X>
S Brezinsek  <https://orcid.org/0000-0002-7213-3326>
B Unterberg  <https://orcid.org/0000-0003-0866-957XL>
Ch Linsmeier  <https://orcid.org/0000-0003-0404-7191>

References

- [1] Brezinsek S *et al* 2017 Plasma-wall interaction studies within the EUROfusion consortium: progress on plasma-facing components development and qualification *Nucl. Fusion* **57** 116041
- [2] Linsmeier C *et al* 2017 Development of advanced high heat flux and plasma-facing materials *Nucl. Fusion* **57** 092007
- [3] Coenen J W *et al* 2018 Improved pseudo-ductile behavior of powder metallurgical tungsten short fiber-reinforced tungsten (Wf/W) *Nucl. Mater. Energy* **15** 214–9
- [4] Terra A *et al* Micro-structured tungsten: an advanced plasma-facing material *J. Nucl. Mater. Energy* **19** 7–12
- [5] Huber A *et al* 2014 Investigation of the impact of transient heat loads applied by laser irradiation on ITER-grade tungsten *Phys. Scr.* **TS159** 014005
- [6] Wirtz M *et al* 2017 High pulse number thermal shock tests on tungsten with steady state particle background *Physica Scripta* **T170** 014066
- [7] Wirtz M *et al* 2015 *Fusion Sci. Technol.* **68** 8–14
- [8] Kreter A *et al* 2015 Linear plasma device PSI-2 for plasma-material interaction studies *Fusion Sci. Technol.* **68** 8–14
- [9] Möller S *et al* *In situ* investigation of helium fuzz growth on tungsten in relation to ion flux, fluence, surface temperature and ion energy using infrared imaging in PSI-2 *Phys. Scr.* **T170** 014017
- [9] Gago M *et al* 2020 *PFMC-17 Proc.*